International Journal of Nanomedicine

Dovepress
open access to scientific and medical research

Open Access Full Text Article

ORIGINAL RESEARCH

Nanotubular TiO_2 regulates macrophage M2 polarization and increases macrophage secretion of VEGF to accelerate endothelialization via the ERK1/2 and PI3K/AKT pathways

This article was published in the following Dove Medical Press journal:
International Journal of Nanomedicine

Wei-Chang Xu[1,*]
Xiao Dong[1,*]
Jing-Li Ding[2]
Ji-Chun Liu[1]
Jian-Jun Xu[1]
Yan-Hua Tang[1]
Ying-Ping Yi[3]
Chao Lu[1]
Wei Yang[1]
Jue-Sheng Yang[1]
Yi Gong[1]
Jian-Liang Zhou[1]

[1]Department of Cardiovascular Surgery, The Second Affiliated Hospital of Nanchang University, Nanchang, China; [2]Department of Gastroenterology, The Second Affiliated Hospital of Nanchang University, Nanchang, China; [3]Department of Science and Education, The Second Affiliated Hospital of Nanchang University, Nanchang, China

*These authors contributed equally to this work

Correspondence: Jian-Liang Zhou
Department of Cardiovascular Surgery, The Second Affiliated Hospital of Nanchang University, No. 1 Minde Road, Nanchang 330006, Jiangxi, China
Tel +86 137 6711 7511
Email zhoujianliang2010@163.com

Background: Macrophages play important roles in the immune response to, and successful implantation of, biomaterials. Titanium nanotubes are considered promising heart valve stent materials owing to their effects on modulation of macrophage behavior. However, the effects of nanotube-regulated macrophages on endothelial cells, which are essential for stent endothelialization, are unknown. Therefore, in this study we evaluated the inflammatory responses of endothelial cells to titanium nanotubes prepared at different voltages.

Methods and results: In this study we used three different voltages (20, 40, and 60 V) to produce titania nanotubes with three different diameters by anodic oxidation. The state of macrophages on the samples was assessed, and the supernatants were collected as conditioned media (CM) to stimulate human umbilical vein endothelial cells (HUVECs), with pure titanium as a control group. The results indicated that titanium dioxide (TiO_2) nanotubes induced macrophage polarization toward the anti-inflammatory M2 state and increased the expression of arginase-1, mannose receptor, and interleukin 10. Further mechanistic analysis revealed that M2 macrophage polarization controlled by the TiO_2 nanotube surface activated the phosphatidylinositol 3-kinase/AKT and extracellular signal-regulated kinase 1/2 pathways through release of vascular endothelial growth factor to influence endothelialization.

Conclusion: Our findings expanded our understanding of the complex influence of nanotubes in implants and the macrophage inflammatory response. Furthermore, CM generated from culture on the TiO_2 nanotube surface may represent an integrated research model for studying the interactions of two different cell types and may be a promising approach for accelerating stent endothelialization through immunoregulation.

Keywords: TiO_2 nanotubes, axitinib, stent implant, endothelial cells, conditioned medium

Introduction

Heart valve replacement is the main treatment for heart valve disease. However, heart valve stents are prone to thrombosis and have historically presented challenges.[1] Recent research has indicated that rapid re-endothelialization after stent implantation can reduce platelet adhesion and inflammatory responses, thereby decreasing the risk of thrombosis.[2,3] Hence, surface modification of stent materials is a promising method to accelerate endothelialization.

Heart valve stents play a crucial role in the anatomy reconstruction of tissue damage in heart valve replacement surgery, and the performance of implantable stents has a considerable impact on material–host interactions. Titanium is the most commonly

submit your manuscript | www.dovepress.com
Dovepress
http://dx.doi.org/10.2147/IJN.S188439

used metallic material for heart valve stents, whose superior biocompatibility is related to the layer of titanium dioxide (TiO_2).[4] Nanotechnology has been widely used in surface modification of materials. The nanostructure morphology on the surface of implanted materials can affect the morphology and function of adherent cells[5] and can regulate cell behavior as a drug nanoreceptor.[6] Moreover, TiO_2 nanotubes can reduce the inflammatory response of macrophages by inhibiting the nuclear factor-κB (NF-κB) pathway,[7] and TiO_2 is easily formed on the material surface through a simple electrochemical process.[8,9] Interestingly, highly ordered TiO_2 nanotubes with a diameter of about 70 nm improve human umbilical vein endothelial cell (HUVEC) adhesion, proliferation, and angiogenesis,[10] indicating that the morphology of biomaterials is relevant to bodily responses. Although endothelial cells can be guided by titanium nanotubes,[11–13] the interaction between the effects of nanotubes on macrophages and the functions of endothelial cells remains unclear.

Unfortunately, common biomaterials (eg, bioceramic and titanium) have adverse influences on tissues and cells in vivo and in vitro.[14,15] Host immune responses may have a negative impact on recovery and can target implanted biomaterials. When metallic implants are applied, various proteins will adhere to the implants, subsequently inducing a host inflammatory response and initiating endothelial repair. Slight inflammation is necessary, and the environment around the implant material is affected by the inflammatory response.[16] Although it is believed that proper inflammation facilitates the recruitment of endothelial cells from the surrounding environment, excessive or persistent inflammation activates downstream pathways, leading to delayed tissue healing and inflammatory damage.[17,18] Macrophages and their precursor monocytes, as pivotal players in innate immunity, are largely involved in the development and progression of inflammation, directly related to M1/M2 polarization of macrophages. M1 macrophages promote inflammation, whereas M2 macrophages inhibit inflammation.[19] Different tissue microenvironments induce macrophage polarization and various cytokines will be secreted in response. M1 macrophages synthesize tumor necrosis factor alpha (TNF-α), interleukin-1β (IL-1β), IL-8, inducible nitric oxide synthase (iNOS), C-C chemokine receptor type 7 (CCR7), and others.[20,21] M2 macrophages produce arginase-1 (ARG1), mannose receptor (CD206), and IL-10[22] as well as vascular endothelial growth factor (VEGF),[23,24] which supports the homing, migration, and proliferation of endothelial cells.[25] Therefore, further studies are needed to investigate the promotion/inhibition of HUVEC behaviors by the mixture secreted by macrophages on the surface of TiO_2 nanotubes.

Accordingly, in this study, we evaluated the inflammatory response to commercially pure Ti (CP) and to TiO_2 nanotubes generated using 20 (TNT20), 40 (TNT40), and 60 V (TNT60). The objective of this study was to elucidate the effects and mechanisms of nanotube-based implants, macrophage polarization, and endothelialization. The results are expected to establish a complete model for assessing the characterization of heart valve stent materials and provide a promising method to accelerate stent endothelialization via immunomodulation.

Materials and methods

Nanotubular TiO_2 preparation and characterization

Pure titanium (Baoti, Baoji, China) was used to fabricate circular pieces with a diameter of 34 mm and thickness of 1 mm as raw materials. We employed the anodic oxidation method to treat the Ti plates.[26] The Ti plates were cleaned with ethanol, acetone, and double distilled water via ultrasonic treatment. Then, polishing water containing HF, HNO_3, and H_2O (volume ratio: 1:4:5) was used to polish the Ti plates for 1 minute. The Ti plates were placed in electrolyte solution composed of HF and ethylene glycol for 60 minutes under different voltages (20, 40, and 60 V). A Ti plate that was not subjected to electrolysis was used as a control. Before seeding cells, the plates were exposed to ultraviolet radiation for 1 hour.

The surface morphology and topography of the Ti samples were characterized by scanning electron microscopy (SEM; JEOL JSM-6700F, Tokyo, Japan). The surface wettability of each sample was examined using a contact angle meter (DMCE1; Niiza, Japan).

Cell culture

Two cell types, THP1 human monocytic cells and HUVECs, were cultured. THP1 cells were purchased from the cell bank of the Chinese Academy of Sciences, and HUVECs were purchased from American Type Culture Collection (ATCC, Manassas, VA, USA). THP1 cells were cultivated in RPMI medium containing 10% FBS under standard conditions (5% CO_2, 37°C, and 100% humidity). Before use, THP1 cells were treated with phorbol myristate acetate (PMA, 100 ng/mL). The cells were then seeded on Ti plates treated at TNT20, TNT40, and TNT60, and pure Ti plates were used as a control. After 3 days, culture medium was collected and mixed with complete DMEM at a ratio of 1:1 to prepare conditioned medium (CM). HUVECs were cultivated in DMEM containing 10% FBS

under standard conditions (5% CO_2, 37°C, and 100% humidity). When cells were approximately 80% confluent, they were subcultured using 0.25% trypsin-EDTA.

Behaviors of macrophages on nanotubular Ti surfaces

Observation of macrophage morphology

THP1 cells were seeded onto different Ti plates in 24-well plates (1×10^5 cells/mL) and cultured for 3 days. Next, 50 ng/mL IL-4 was added as a positive control group. For SEM imaging, all samples were rinsed twice with PBS and fixed in 2.5% glutaraldehyde overnight at 4°C. Then, samples were dehydrated using increasing concentrations of ethanol. All cells were finally dehydrated with hexamethyldisilazane and air-dried for 40 minutes. All samples were sputter-coated with gold before SEM.

Macrophage polarization analysis

Prior to confocal laser scanning microscopy (CLSM) observation, macrophage polarization was studied using indirect immunofluorescence staining. Rabbit antihuman CD86 (1:500; Abcam, Cambridge, UK) was used as a pro-inflammatory marker, and rat antihuman CD206 (1:50; Abcam) was used as an anti-inflammatory marker. THP1 cells were treated with PMA (100 ng/mL) and then seeded on Ti plates for 48 hours. The cells were fixed in paraformaldehyde at 4°C for 10 minutes and subsequently treated with 0.1% Triton X-100 (Sigma-Aldrich, Shanghai, China) for 10 minutes. After being blocked with normal goat serum, the cells were incubated with primary antibodies at 4°C overnight. Next, donkey anti-rabbit IgG (Alexa Fluor 488; 1:100; Abcam) and donkey anti-rat IgG (Alexa Fluor 488; 1:100; Abcam) secondary antibodies were used to visualize the cells. The nuclei were stained with DAPI, and all samples were observed by CLSM. Flow cytometry was used to detect the polarization of macrophages. The macrophages on the samples were collected by trypsinization. Next, samples were fixed with 4% paraformaldehyde for 10 minutes and then blocked with 10% goat serum for 30 minutes. Samples were incubated with rabbit antihuman CD86 (1:100; Abcam) and rat antihuman CD206 (1:50; Abcam) antibodies for 30 minutes, washed with precooled PBS three times (5 minutes each), and incubated with fluorescently labeled secondary donkey anti-rabbit IgG (Alexa Fluor 488; 1:200; Abcam) or donkey anti-rat IgG (Alexa Fluor 488; 1:200; Abcam) for 30 minutes in the dark. After washing three times with PBS, samples were detected by flow cytometry (BD LSRFortessa; BD, Franklin Lakes, NJ, USA).

Expression of inflammation-associated proteins

Western blotting was performed for detection of NF-κB pathway signaling molecules. Cells were lysed with radioimmunoprecipitation assay buffer. Approximately 20–40 μg of each cell extract was separated by electrophoresis and transferred to polyvinylidene difluoride membranes. Next, 5% skim milk was used to block the membranes for 1 hour, followed by incubation with primary antibodies overnight. Membranes were then washed three times and incubated with secondary antibodies for 1 hour at room temperature. Finally, membranes were developed using enhanced chemiluminescence. Blots were exposed to Tanon (Shanghai, China).

Subsequently, pro-inflammatory cytokines (TNF-α, IL-1β, and IL-8) were examined with chemiluminescence. Macrophage supernatants were collected and then analyzed with IMMULITE 1000 TNF-α, IL-1β, and IL-8 kits (Siemens Inc., Los Angeles, CA, USA), according to the manufacturer's instructions. The detection limits of the assays were 0.12–1,000 pg/mL for TNF-α, 1.5–1,000 pg/mL for IL-1β, and 2–7,500 pg/mL for IL-8.

RNA isolation and quantitative real-time PCR analysis

Total RNA was extracted using an RNeasy Mini Kit (QIAGEN, Hilden, Germany) according to the manufacturer's instructions. Five M1-related genes, ie, *IL-1β*, *IL-8*, *iNOS*, *CCR7*, and *TNF-α*, and three M2-related genes, ie, *ARG1*, *CD206*, and *IL-10*, were detected by quantitative real-time PCR using a Bio-Rad Quantitative System (Hercules, CA, USA). In addition, the mRNA levels of *VEGF* were detected. Relative gene expression was normalized to the housekeeping gene glyceraldehyde 3-phosphate dehydrogenase (*GAPDH*). The PCR primers used are listed in Table 1 (Sangon Biotech, Shanghai, China).

Endothelialization rate in CM

HUVEC adhesion and proliferation assay

HUVECs were cultured in 96-well tissue culture plates with 2×10^5 cells/mL in CM. After 2, 4, or 12 hours, wells were rinsed with PBS three times. The adherent cells were cultured with Cell Counting Kit-8 solution (Dojindo, Kumamoto, Japan) for 2 hours and read with a 450 nm filter.

To investigate the proliferation of HUVECs in different CM, cells were seeded at 2×10^4 cells/mL in a 96-well tissue culture plate. After 1, 3, or 5 days, 10 μL CCK8 solution was added to each well, and cells were incubated for 2 hours, after which the absorbance at 450 nm was measured using a microplate reader.

Table 1 Primers used in this study

Gene and primer direction	Sequence
Human *GAPDH*	
Forward	5′-TGAAGGTCGGAGTCAACGG-3′
Reverse	5′-AGAGTTAAAAGCAGCCCTGGTG-3′
Human *ARG1*	
Forward	5′-GTGGAAACTTGCATGGACAAC-3′
Reverse	5′-AATCCTGGCACATCGGGAATC-3′
Human *CD206*	
Forward	5′-TCCGGGTGCTGTTCTCCTA-3′
Reverse	5′-CCAGTCTGTTTTTGATGGCACT-3′
Human *IL-10*	
Forward	5′-GTTGTTAAAGGAGTCCTTGCTG-3′
Reverse	5′-TTCACAGGGAAGAAATCGATGA-3′
Human *IL-1β*	
Forward	5′-ATGATGGCTTATTACAGTGGCAA-3′
Reverse	5′-GTCGGAGATTCGTAGCTGGA-3′
Human *IL-8*	
Forward	5′-TTTTGCCAAGGAGTGCTAAAGA-3′
Reverse	5′-AACCCTCTGCACCCAGTTTTC-3′
Human *TNF-α*	
Forward	5′-CCTCTCTCTAATCAGCCCTCTG-3′
Reverse	5′-GAGGACCTGGGAGTAGATGAG-3′
Human *CCR7*	
Forward	5′-TGAGGTCACGGACGATTACAT-3′
Reverse	5′-GTAGGCCCACGAAACAAATGAT-3′
Human *iNOS*	
Forward	5′-TTCAGTATCACAACCTCAGCAAG-3′
Reverse	5′-TGGACCTGCAAGTTAAAATCCC-3′
Human *VEGF*	
Forward	5′-ATCGAGTACATCTTCAAGCCAT-3′
Reverse	5′-GTGAGGTTTGATCCGCATAATC-3′
Human *ITGAV*	
Forward	5′-ACAGGCAATAGAGATTATGCCA-3′
Reverse	5′-TTTATCCTGTTTCGACCTCACA-3′
Human *vWF*	
Forward	5′-CCGATGCAGCCTTTTCGGA-3′
Reverse	5′-TCCCCAAGATACACGGAGAGG-3′

Abbreviations: *ARG1*, arginase-1; *CCR7*, C-C chemokine receptor type 7; *CD206*, mannose receptor; *GAPDH*, glyceraldehyde-3-phosphate dehydrogenase; *IL*, interleukin; *ITGAV*, integrin subunit alpha V; *TNF-α*, tumor necrosis factor α; *VEGF*, vascular endothelial growth factor; *iNOS*, inducible nitric oxide synthase; *vWF*, von Willebrand factor.

HUVEC angiogenic determination

Scratch assays were conducted to analyze endothelial cell migration ability. HUVECs were seeded in 6-well plates, and when cells reached 100% confluence, the cell monolayer was carefully scratched with a pipette and then washed with PBS three times. Next, CM was added, and images were acquired at 0 and 6 hours after the cells were scratched. ImageJ software (Rawak Software Inc., Stuttgart, Germany) was used to evaluate the area of the scratch.

When HUVECs are grown on Matrigel (BD Biosciences, San Jose, CA, USA), they spontaneously form capillary-like structures. In tube formation assays, 96-well plates were coated with 50 μL Matrigel and incubated at 37°C for 30 minutes. HUVECs were seeded at a density of 4×10^5/mL with 100 μL CM and imaged after incubation for 6 hours. ImageJ software was used to analyze the number of branch points and total tube length per field. According to a previous description,[27,28] the mRNA levels of von Willebrand factor (*vWF*) and integrin subunit alpha V (*ITGAV*) were detected.

Mechanism of HUVEC endothelialization

A human VEGF ELISA kit (Multi Sciences, Hangzhou, China) was used to analyze VEGF content in the supernatants of macrophages cultured on Ti plates. According to the manufacturer's instructions, all reagents and working standards were prepared, mixed with 50 μL sample, and incubated for 2 hours at room temperature. After aspiration and washing six times, 100 μL diluted streptavidin-horseradish peroxidase was added to each well, and plates were incubated for 45 minutes at room temperature. Following aspiration and washing six times, 100 μL substrate solution was added to each well. Finally, 100 μL stop solution was added, and the absorbance was read at 450 nm.

To determine whether VEGF was involved in the regulation of endothelialization, 1 μM of the VEGF receptor antagonist axitinib (Selleck, Houston, TX, USA) was added to the endothelial cell culture medium. Cells were incubated for 24 hours, and CM was then added, followed by observation of endothelialization. Activation of the extracellular signal-regulated kinase 1/2 (ERK1/2) and phosphatidylinositol 3-kinase (PI3K)/AKT pathways was detected by Western blotting. PD98059 (an ERK1/2 inhibitor) and LY294002 (an AKT inhibitor) were also added to the medium to verify the influence of the ERK1/2 and AKT pathways.

Statistical analysis

The data were analyzed with GraphPad Prism7 (GraphPad Software, Inc., La Jolla, CA, USA) and presented as the mean ± SD. Significant differences were identified using one-way analysis of variance. Probability values of less than 0.05 were considered significant.

Results

Characterization of nanotubular TiO_2 surfaces

Surface morphology

After anodization at several voltages (20, 40, and 60 V), the TiO_2 nanotubular surfaces were characterized by

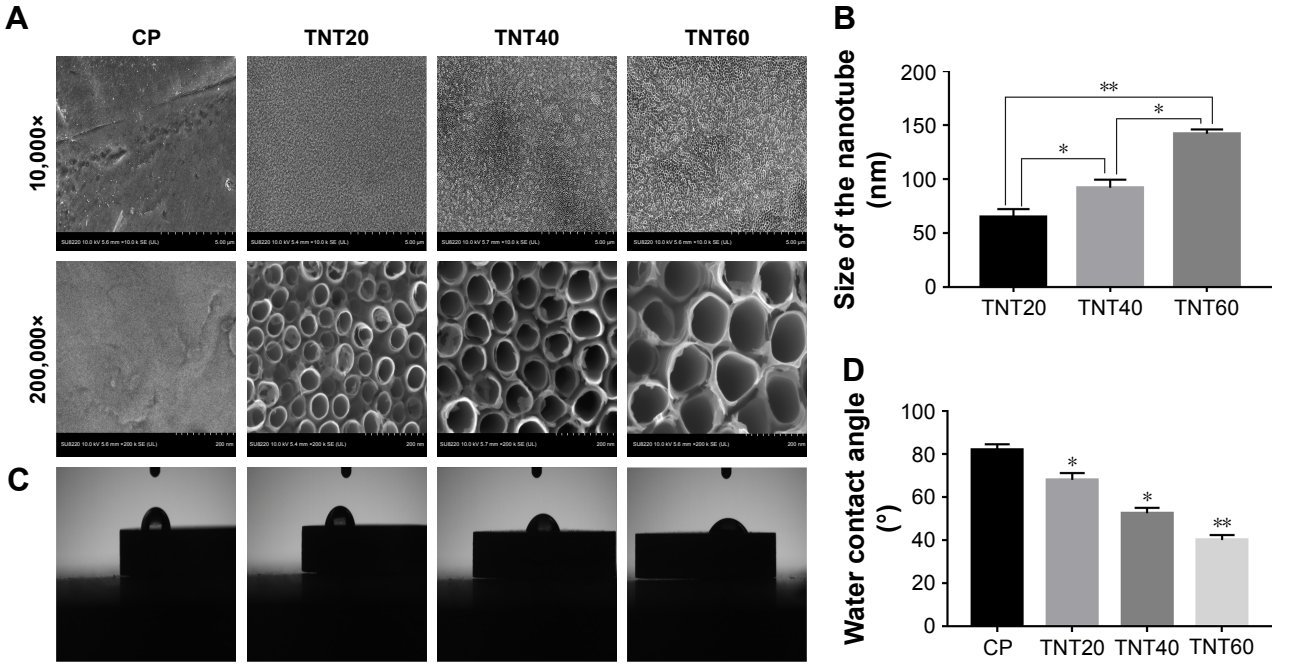

Figure 1 Characterization of nanotubular TiO_2 surfaces.
Notes: (**A**) The surface morphologies of four samples (CP, TNT20, TNT40, and TNT60) observed using SEM at different magnifications. (**B**) The diameters of the nanotubes. (**C**) Images of the water contact angles of samples. (**D**) Analysis of water contact angles in **C**. Results are presented as mean ± SD (N=3). *$P<0.05$, **$P<0.01$.
Abbreviations: CP, commercially pure Ti; TNT20, TiO_2 nanotubes generated using 20 V; TNT40, TiO_2 nanotubes generated using 40 V; TNT60, TiO_2 nanotubes generated using 60 V; SEM, scanning electron microscopy. 10,000×, magnified 10,000 times. 200,000×, magnified 200,000 times.

SEM (Figure 1A). The diameter of the nanotubes increased with increasing voltage but was largely consistent at each voltage. As shown in Figure 1B, the diameters of the nanotubes were 65±7.6 (20 V), 92±7.5 (40 V), and 142±4.0 nm (60 V).

Surface wettability

Wetting angle measurements are shown in Figure 1C. The contact angles of the water droplets on the CP, TNT20, TNT40, and TNT60 samples were 82°±3°, 68°±3°, 52.5°±2.5°, and 40°±2.4°, respectively (Figure 1D).

Macrophage behavior on nanotubular TiO_2 surfaces

Cell morphology

Macrophage morphology on different nanotubular TiO_2 surfaces was observed by SEM. The macrophages displayed distinct shapes on the varying surfaces. Macrophages on CP stretched rapidly and exhibited an oval shape, whereas those on TNT20, TNT40, and TNT60 appeared obviously elongated. The morphology of macrophages on titanium nanotubes was similar to that of the positive control group (Figure 2A). Under high magnification, macrophages were observed with long and abundant pseudopodia on the TNT20, TNT40, and TNT60 samples. The elongated shape was consistent with the morphology of M2 macrophages.

Macrophage polarization analysis

Confocal images showed that the CP group had stronger fluorescence when the sample was incubated with the M1-related anti-CD86 antibodies (Figure 2B). When anti-CD206 antibodies were used, the fluorescence of the titanium nanotube group was stronger, consistent with the results in the positive control group supplemented with IL-4 (Figure 2C). Flow cytometry also showed a large positive ratio of the macrophage M1 marker protein (CD86) on CP and a large fluorescence positive ratio of the macrophage M2 marker protein (CD206) on TNT20, TNT40, and TNT60 (Figure 2D). Digitization of the images (Figure 2E and F) suggested that the surface structures of Ti implants influenced macrophage shape and indicated that the TiO_2 nanotubes promoted M2 macrophage polarization.

Inflammatory response of macrophages

RT-PCR revealed the level of M1 polarization- and M2 polarization-related genes (Figure 2G). With M1 polarization, *IL-1β*, *IL-8*, *TNF-α*, *CCR7*, and *iNOS* expression was high. In contrast, high *ARG1*, *CD206*, and *IL-10* expression represented M2 polarization. Chemiluminescence was used to detect the release of inflammatory factors, and Western blotting was used to detect the activation of inflammation-related pathways. Inflammatory factors (IL-1β, IL-8, and TNF-α) in

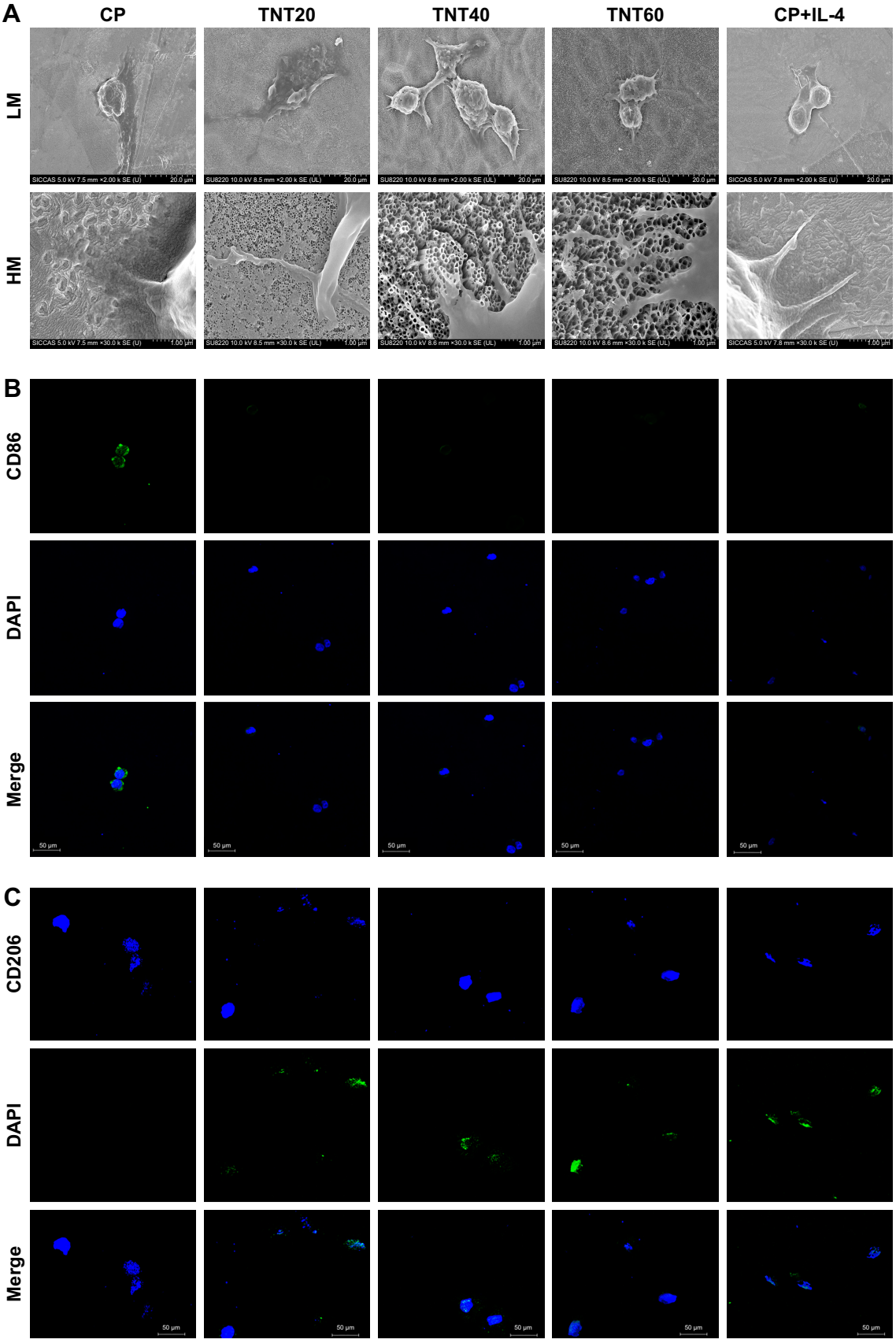

Figure 2 (*Continued*)

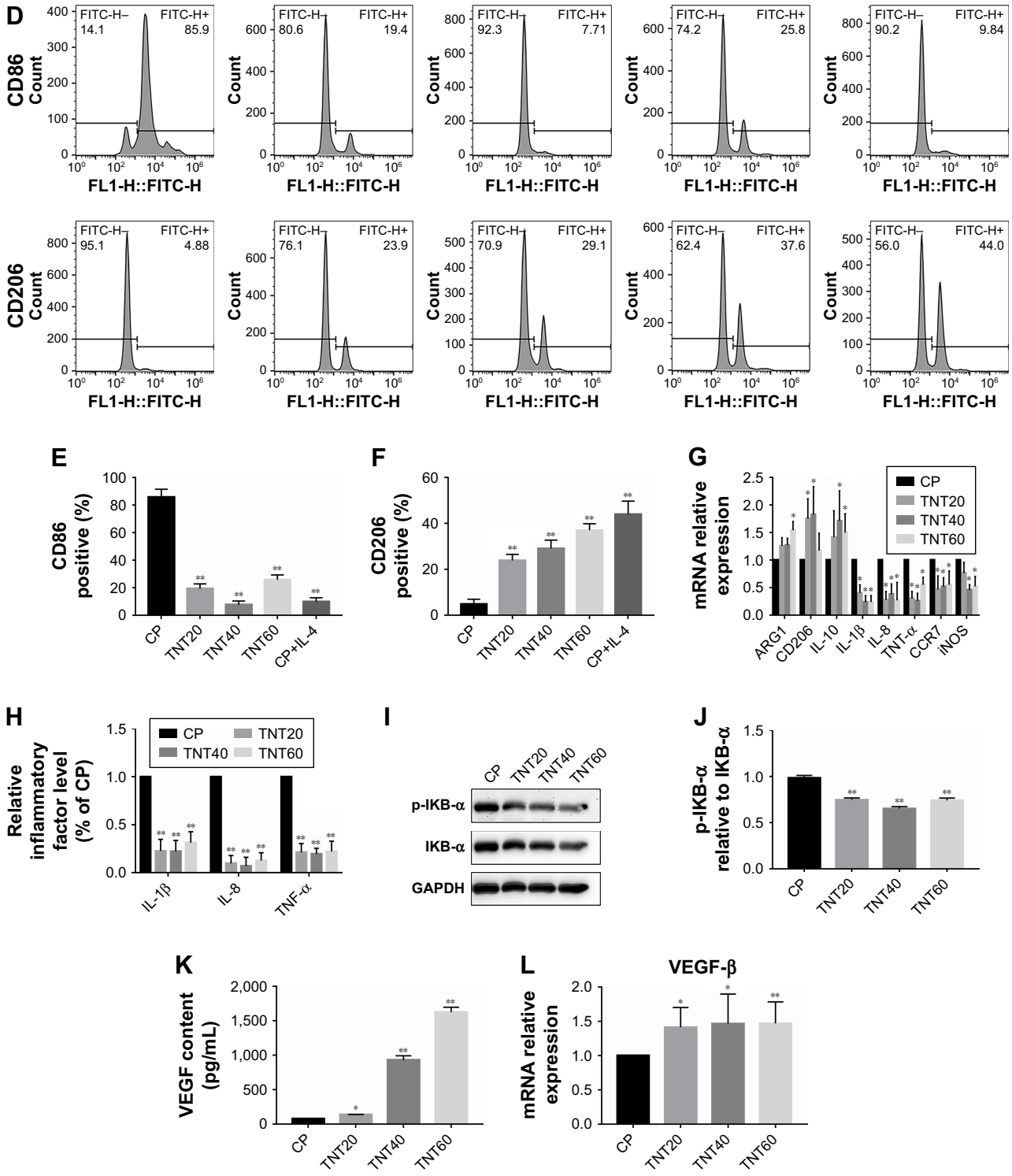

Figure 2 Macrophage behavior on nanotubular TiO_2 surface.

Notes: (**A**) SEM of macrophages incubated for 3 days on different samples (CP, TNT20, TNT40, and TNT60). (**B**) Confocal detection of the M1 marker protein CD86 after 48 hours of culture. (**C**) Confocal detection of the M2 marker protein CD206 after 48 hours of culture. (**D**) Flow cytometry for detection of the membrane surface proteins CD86 and CD206. (**E**) Analysis of flow cytometry results for CD86-positive rates. (**F**) Analysis of flow cytometry results for CD206-positive rates. (**G**) Real-time PCR detection of macrophage polarization and inflammation-related gene expression after 24 hours of culture. (**H**) Chemiluminescence detection of inflammatory factors in supernatants. (**I**) Western blot analysis of inflammation-related proteins on CP, TNT20, TNT40, and TNT60 after 20 minutes of culture. (**J**) Analysis of phospho-IKB-α activity using the images shown in **I**. (**K**) ELISA of macrophage-secreted VEGF in supernatants after 72 hours of culture. (**L**) *VEGF* gene expression levels in macrophages after 24 hours of culture. Results are presented as mean ± SD (N=3). *$P<0.05$; **$P<0.01$.

Abbreviations: CP, commercially pure Ti; TNT20, TNT40, and TNT60, TiO_2 nanotubes produced by different voltages; VEGF, vascular endothelial growth factor; SEM, scanning electron microscopy; LM, low magnification; HM, high magnification; PCR, polymerase chain reaction.

the TNT20, TNT40, and TNT60 supernatants were reduced compared with those in the CP supernatants (Figure 2H). The levels of phospho-IKB-α, part of a traditional inflammatory pathway, were decreased in the TNT20, TNT40, and TNT60 groups compared with that in the CP group (Figure 2I and J). Our data revealed that TiO_2 nanotubes caused less inflammation than CP.

Through ELISA and RT-PCR, we found that the macrophages secreted more VEGF when seeded on TiO_2 nanotubes (Figure 2K), and TiO_2 increased *VEGF* gene expression compared with CP (Figure 2L). Taken together, these data demonstrated that macrophages tended toward M2 polarization on TiO_2 nanotubes and secreted more VEGF, which could lead to regulation of endothelial cell behavior.

In vitro acceleration of endothelialization by macrophages on nanotubular TiO_2 surfaces

Effects of macrophage CM on endothelialization of HUVECs

A schematic diagram based on the cell culture model is shown in Figure 3. Cell migration, tube formation, proliferation, adhesion, and expression of endothelialization-related genes were evaluated to determine the endothelialization speed induced by nanotubular TiO_2 surfaces via macrophages. As shown in Figure 4A, CM from TNT20 (CM20), TNT40, and TNT60 significantly enhanced cell migration. For HUVECs treated with CM from CP, only 45.47% of the wound was closed after 6 hours, whereas for those treated with CM from TNT20, TNT40, and TNT60, wound closure rates were 59.12%, 60.26%, and 69.86%, respectively (Figure 4B). Additionally, we observed apparent capillary-like networks in all groups except the CP group (Figure 4C). Moreover, quantitative analysis revealed a significant increase in the number of new tubes and total tube length of HUVECs cultured in CM from all Ti samples (CP< TNT20< TNT40< TNT60; Figure 4D and E). As shown in Figure 4F and G, cell proliferation and adhesion were evaluated using CCK-8 assays. Cell density significantly increased after cell culture for 3 days in CM from TNT20, TNT40, and TNT60 compared with that in cells cultured in CM from CP. All TNT20, TNT40, and TNT60 samples improved HUVEC adhesion after cultivation for 12 hours when compared with that on CP. Further exploration of the expression levels of the endothelial markers *ITGAV* and *vWF* was carried out by RT-PCR at 24 hours after culture in CM from different samples. The expression levels of both genes were increased in CM from TNT60 compared with those in CM from CP (Figure 4H). Furthermore, the mRNA level of *ITGAV* in macrophages cultured on TNT20 and TNT40 was slightly increased when compared with that on CP.

Overall, these results demonstrated that all CM from TiO_2 nanotubes (TNT20, TNT40, and TNT60) accelerated in vitro endothelialization of HUVECs, particularly the TNT60 TiO_2 nanotubes, compared with CM from CP.

Effects of axitinib on endothelialization of HUVECs

We observed high expression of *VEGF* in macrophages that were seeded on nanotubular TiO_2 surfaces. In order to verify the effects of VEGF on HUVECs, we added axitinib, an efficacious inhibitor of VEGF, to CM prior to culture of HUVECs. As shown in Figure 5A–C, when axitinib was added, the migration and tube formation ability of HUVECs were almost nonexistent. In the cell proliferation assay (Figure 5D), the density of HUVECs with axitinib added to the CM was significantly reduced compared with that of HUVECs cultured in only CM. In addition, the results showed that HUVEC density remained low and increased slowly when axitinib was added. Furthermore, axitinib affected the activation of the ERK1/2 and PI3K/AKT

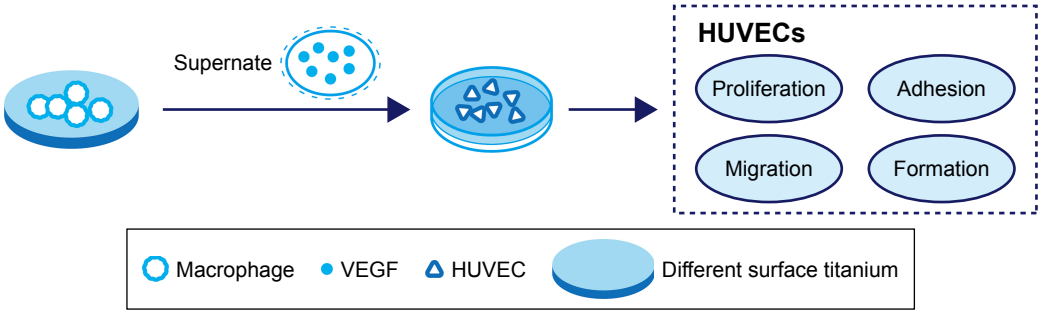

Figure 3 Schematic of cell culture model.
Note: Effects of macrophage supernatants on HUVECs tested under in vitro conditions.
Abbreviations: VEGF, vascular endothelial growth factor; HUVEC, human umbilical vein endothelial cell.

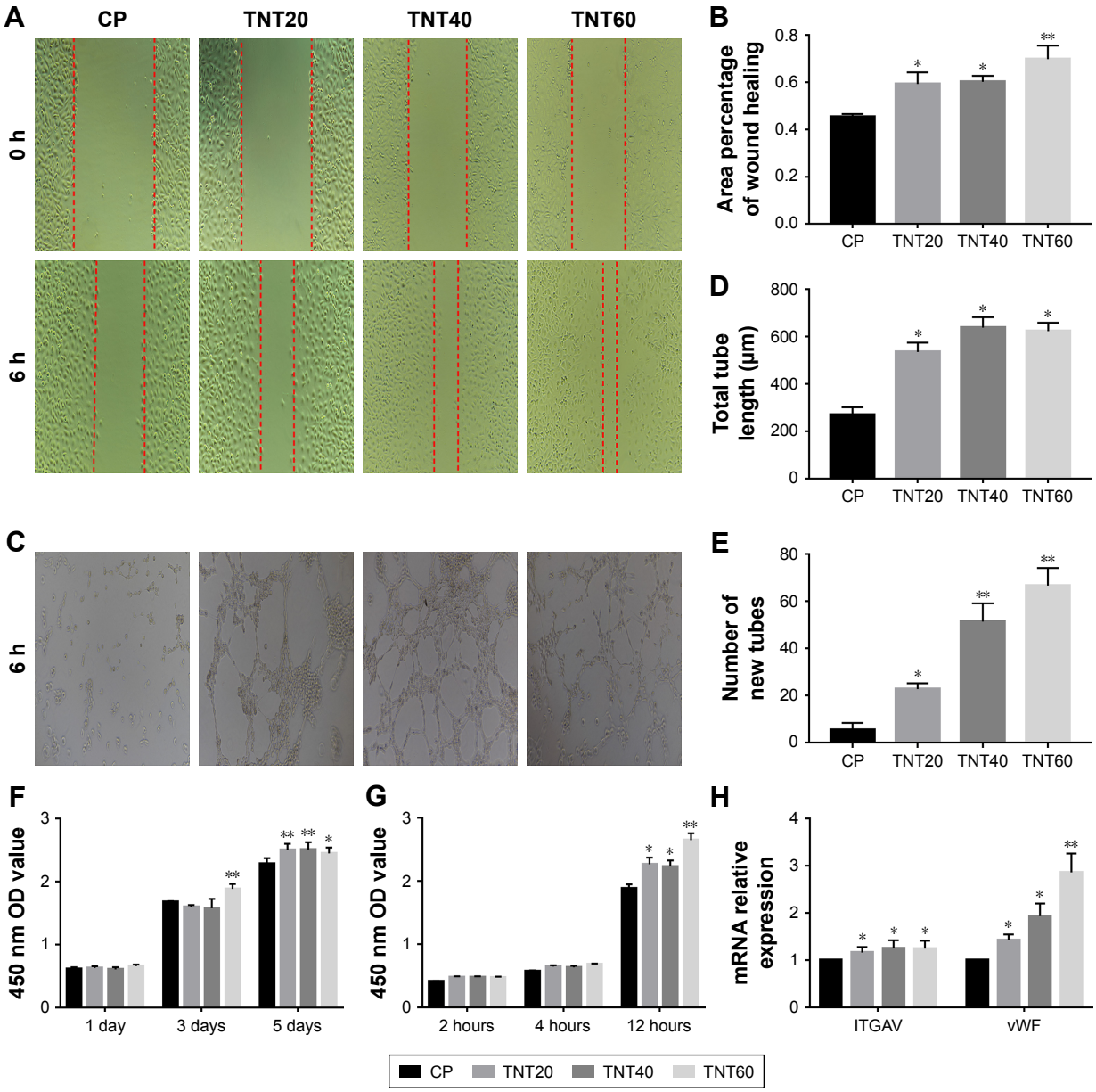

Figure 4 Evaluation of the in vitro behaviors of HUVECs stimulated with conditioned medium.

Notes: (**A**) Representative images of HUVEC migration. (**B**) The percentage of coverage after 6 hours of wound healing. (**C**) Representative images of tube formation for 6 hours. (**D**) Quantitative analysis of the lengths of new tubes. (**E**) Quantitative analysis of the number of new tubes. (**F**) Cell proliferation in HUVECs for 1, 3, and 5 days. (**G**) Cell adhesion in HUVECs after 2, 4, and 12 hours. (**H**) Relative expression of the *ITGAV* and *vWF* genes in HUVECs after incubation in macrophage CM for 24 hours. Results are presented as means ± SD (N=3). $^*P<0.05$; $^{**}P<0.01$.

Abbreviations: HUVEC, human umbilical vein endothelial cell; CP, TNT20, TNT40, and TNT60, conditioned medium from commercially pure Ti or TiO_2 nanotubes produced by 20, 40, or 60 V; ITGAV, integrin alpha chain V; vWF, von Willebrand factor.

pathways (Figure 5E and F). Axitinib slightly reduced the phosphorylation of AKT and significantly reduced the phosphorylation of ERK1/2. The addition of 100 nm and 1 μm axitinib reduced the phosphorylation of AKT, whereas 10 nm, 100 nm, and 1 μm axitinib reduced the phosphorylation of ERK1/2. These findings suggested that when VEGF inhibitor was added to CM, the CM did not accelerate endothelialization. Thus, VEGF was found to be important for CM-accelerated endothelialization and may function through the ERK1/2 and PI3K/AKT pathways.

Effects of HUVEC stimulation with CM on the ERK1/2 and AKT pathways

Scratch, tube formation, and cell proliferation assays were performed to assess endothelialization when CM (from TNT60 TiO_2 nanotubes) contained PD98059 and LY294002.

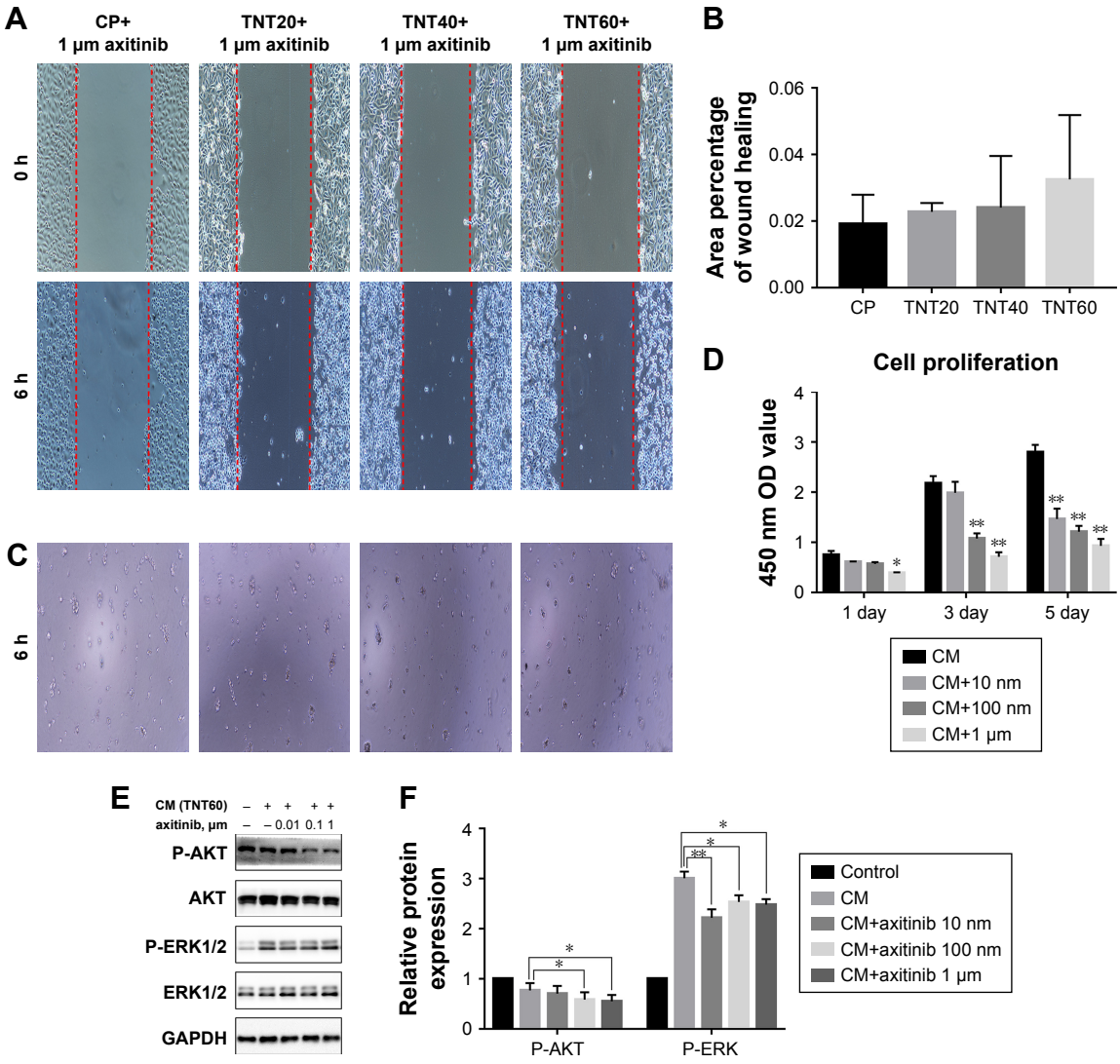

Figure 5 Axitinib inhibited endothelialization.

Notes: (**A**) Representative images of HUVEC migration. (**B**) The percentage of coverage after 6 hours of wound healing. (**C**) Representative images of tube formation for 6 hours. (**D**) Cell proliferation in HUVECs for 1, 3, and 5 days. (**E**) Determination of AKT and ERK1/2 phosphorylation in HUVECs by Western blotting. (**F**) Analysis of AKT and ERK1/2 phosphorylation using the images shown in **E**. Results are presented as mean ± SD (N=3). *$P<0.05$, **$P<0.01$.

Abbreviations: HUVEC, human umbilical vein endothelial cell; CP, TNT20, TNT40, and TNT60, conditioned medium from commercially pure Ti or TiO_2 nanotubes produced by 20, 40, or 60 V; CM, conditioned medium.

When PD98059 (20 μm), LY294002 (20 μm), or LY294002 (20 μm)+ PD98059 (20 μm) were added to CM (TNT60), migration and tube formation were impaired (Figure 6A–C). Moreover, these inhibitors suppressed HUVEC proliferation (Figure 6D). Western blot assays were then performed to evaluate the phosphorylation of ERK1/2 and AKT. As shown in Figure 6E and F, CM (TNT60) clearly activated ERK1/2 and AKT phosphorylation. In contrast, when PD98059 (ERK1/2 inhibitor, 20 μm) and LY294002 (AKT inhibitor, 20 μm) were added to CM (TNT60), the phosphorylation levels of ERK1/2 and AKT were obviously reduced. A schematic of the VEGF signaling pathway acting on endothelialization is presented in Figure 7. These data verified that CM from TiO_2 nanotubes may accelerate endothelialization through VEGF-activated phosphorylation of ERK1/2 and AKT.

Discussion

The immune system is important for the success of implants.[29] When an implant is introduced to the body, a sequence of immune responses and tissue recovery processes, including a range of vascular, muscular, and cellular responses, occur in the surrounding tissue.[30] In all of these events, macrophages play an essential role in identifying and adhering to the foreign material in addition to secreting chemokines, growth factors, and cytokines, which direct tissue formation

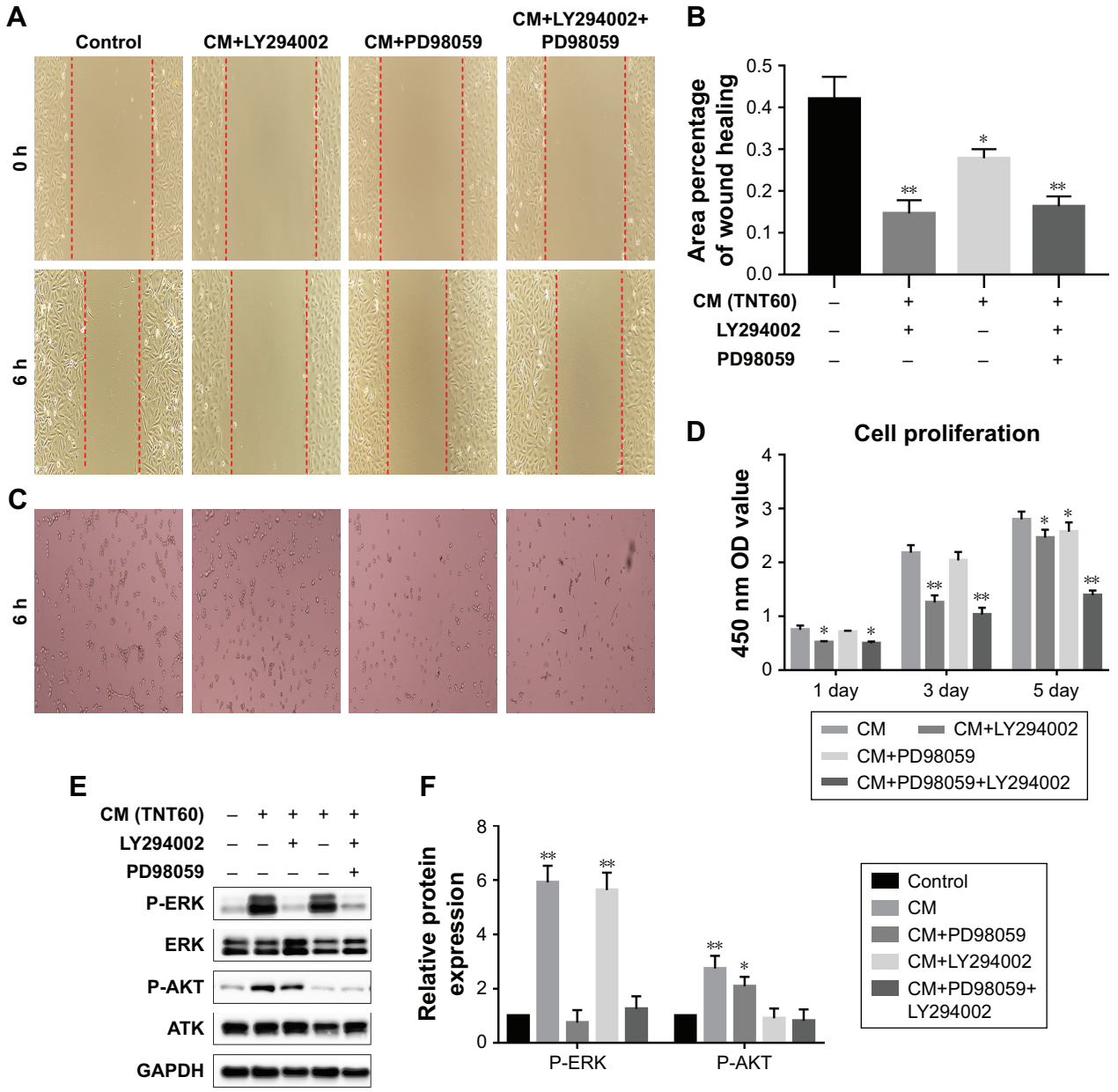

Figure 6 Effects of AKT and ERK1/2 pathway inhibitors on endothelialization.

Notes: (**A**) Representative images of HUVEC migration. (**B**) The percentage of coverage after 6 hours of wound healing. (**C**) Representative images of tube formation for 6 hours. (**D**) Cell proliferation in HUVECs for 1, 3, and 5 days. (**E**) Determination of AKT and ERK1/2 phosphorylation in HUVECs by Western blot. (**F**) Analysis of AKT and ERK1/2 phosphorylation using the images shown in **E**. Results are presented as mean ± SD (N=3). *$P<0.05$, **$P<0.01$.

Abbreviations: LY294002, AKT pathway inhibitor; PD98059, ERK1/2 pathway inhibitor; HUVEC, human umbilical vein endothelial cell; CP, TNT20, TNT40, and TNT60, conditioned medium from commercially pure Ti or TiO_2 nanotubes produced by 20, 40, or 60 V; CM, conditioned medium.

and repair.[31,32] Macrophages are the first cells to reach the tissue/implant interface and identify the foreign matter.[33] Histological studies have shown that macrophages and multinucleated cells are present at the stent interface of Ti implants in the early stages of implantation.[34,35] Inappropriate macrophage activation may exacerbate inflammation and destroy healthy tissue/implant integration, and proper responses to implant surfaces have been shown to be beneficial for tissue healing and implant performance.[35,36] However, heart valve stent thrombosis is a fatal side effect. Fortunately, some research has shown that rapid re-endothelialization can substantially decrease thrombosis risk.[2,37,38] In animal experiments with vascular injury, exfoliation of endothelial cells leads to thrombosis of platelets.[38] Endothelial cell growth, including proliferation, attachment, migration, survival, and secretion of products on the valve, plays a crucial role in preventing blood clotting.[39] Thus, rapid growth of endothelial cells after stent implantation may be beneficial for patients

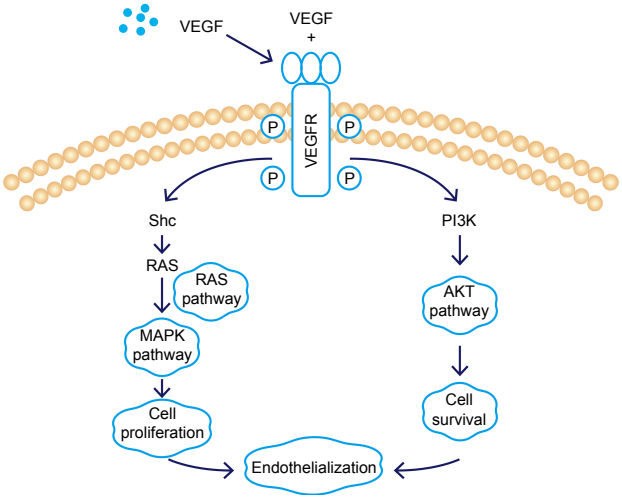

Figure 7 Schematic of the VEGF signaling pathway acting on endothelialization.
Abbreviations: VEGF, vascular endothelial growth factor; VEGFR, vascular endothelial growth factor receptor; Shc, src homology 2 domain containing; RAS, family of related proteins.

undergoing stent therapy. In this study, we observed the influence of TiO_2 nanotube topography on the activation of macrophages, their paracrine interactions with HUVECs, and the specific mechanisms involved. We demonstrated that TiO_2 nanotube surfaces were capable of manipulating macrophage polarization and secretion of VEGF, which led to proper endothelialization via the ERK1/2 and PI3K/AKT pathways.

Our results revealed that the TiO_2 nanotube surfaces (TNT20, TNT40, and TNT60) changed macrophage morphology. Macrophages on CP exhibited an egg-shaped morphology that was representative of M1 macrophages. In contrast, macrophages on TiO_2 nanotube surfaces (TNT20, TNT40, and TNT60) displayed a fusiform shape and many extended pseudopods that corresponded to M2 macrophages. McWhorter et al found that M2 macrophages displayed an elongated shape and more pseudopods compared with M1 macrophages.[40] Furthermore, other studies have confirmed that elongated macrophages on the surface of modified biomaterials exhibit the M2 phenotype.[41–43] However, some other studies have demonstrated opposing results.[44] Therefore, future research must investigate the detailed mechanisms through which TiO_2 nanotube surfaces regulate macrophage polarization.

In general, it is believed that the M1 macrophage phenotype is pro-inflammatory and involved in tissue destruction, whereas the M2 macrophage phenotype is anti-inflammatory and involved in tissue regeneration.[45] M1 macrophages with enhanced IL-1, IL-8, TNF-α, CCR7, and iNOS expression indicate delayed tissue healing and heavier inflammatory response.[20,21] IL-1 activates the NF-κB pathway through binding to IL-1R/toll-like receptors, activating interleukin-receptor-associated kinase-1.[46] Tossetta et al found that IL-1 and transforming growth factor can destroy tight junctions of endothelial cells.[47] In addition, excessive secretion of IL-8 impairs endothelial tube growth.[48] Therefore, inhibition of inflammatory factor production on TiO_2 nanotubes in the present study would benefit endothelialization and tissue healing around the implant. Moreover, TiO_2 nanotubes are likely to induce healing-associated M2 polarization with increasing levels of ARG1 and IL-10.[49] These anti-inflammatory factors contribute to the ability of M2 macrophages to improve tissue regeneration. IL-10 can inhibit the activity and production of the pro-inflammatory cytokines described above and can suppress nitric oxide secretion.[50] The TiO_2 nanotube surfaces showed promising results for maintaining the balance of anti-inflammatory and pro-inflammatory cytokines. However, TiO_2 nanotubes of different diameters exhibited different anti-inflammatory capabilities. TNT60 induced in the weakest inflammatory response and secretion of more anti-inflammatory factors compared with TNT20 and TNT40. Thus, our results demonstrated that large-dimension TiO_2 nanotube surfaces reduced pro-inflammatory cytokine release from macrophages and produced an anti-inflammatory microenvironment that favored endothelial cell growth.

To date, many studies have addressed the key roles of Ti implants in anti-inflammatory responses and have emphasized the important role of nanostructured surfaces.[44,51–54] However, most of these studies have focused on the proliferation, adhesion, and secretion of pro-inflammatory cytokines from macrophages on the material.[53–55] Yao et al similarly used different voltages to fabricate nanotube surfaces and found that larger nanotubular surfaces (120 nm) could inhibit the expression and secretion of pro-inflammatory cytokines in macrophages.[54] Our results were consistent with these findings. We suspect that nanotube diameter may affect the hydrophilicity of the surface, thereby altering macrophage polarization. Cultured macrophages produce an anti-inflammatory microenvironment on high-surface-wettability materials, and this function may promote the healing response to biological materials.[56] Acid treatment increases hydrophilicity,[57] and the larger the diameter of Ti nanotubes, the greater the hydrophilicity.[58] The general rule is that a hydrophilic surface is conducive to cell adhesion, growth, and spreading.[59] The charge properties and charge density of the surface of the material have an important effect on cell growth, and in the absence of serum, the adhesion of cells on the surface of positively charged materials increases.[60] This occurs mainly because of the electrostatic interaction

between the surface of the positively charged material and the negatively charged cells, which facilitates cell adhesion.[61] Moreover, some studies have explored macrophage polarization, but the specific correspondence between macrophage polarization and nanotube dimension is still uncertain. In our study, the largest size of TiO_2 nanotubes (TNT60) had the strongest hydrophilicity, and the surface area of the macrophages was the largest. The TNT20 and TNT40 samples also had stronger hydrophilicity than CP, but these results were opposite to those of a study conducted by Ma et al.[44] This difference may be due to the different methods used to form the nanotube surfaces. Furthermore, it was demonstrated that the production and activation of pro-inflammatory factors in macrophages were influenced by Ti surface characteristics, including surface wettability and topography.[56] Thus, further studies are necessary to evaluate how the surface properties of biomaterials are related to the activation of macrophages.

To improve the outcomes of heart valve implants, an appropriate microenvironment that accelerates tissue healing and reduces side effects, such as thrombosis, must be developed. It is not sufficient solely to analyze the polarization of macrophages on the surface of the implant. Investigation of the interactions between macrophages and surrounding cells, such as endothelial cells, will improve our understanding of the roles of macrophages in tissue regeneration. There is ample evidence that activated macrophages and M2 polarization enhance the expression of VEGF.[23,62,63] VEGF is a key regulator of endothelialization and can synergistically enhance tissue regeneration. Among pro-endothelialization factors, VEGF is the most potent identified to date.[64] Our results were consistent with these findings. TiO_2 nanotube supernatants, compared with those of CP, contained more VEGF and promoted HUVEC proliferation, adhesion, migration, and tube formation. Additionally, HUVECs expressed more *ITGAV* and *vWF* when stimulated with the TiO_2 nanotube supernatant. Moreover, when the VEGF inhibitor was added, the endothelialization-accelerating effect of the supernatant disappeared. These results demonstrated that macrophages cultured on TiO_2 nanotubes accelerated endothelialization by secreting VEGF.

Many studies have suggested that VEGF contributes to the migration, proliferation, and angiogenesis of HUVECs via ERK1/2 and PI3K/AKT signaling pathways.[65] VEGF binds to the Ig domain of the extracellular domain of VEGFR2, activates the mitogen-activated protein kinase cascade, and further activates ERK1/2, thereby promoting cell proliferation.[66] VEGF also activates AKT to regulate cell survival.[67] In our study, addition of the ERK1/2 inhibitor PD98059 significantly inhibited cell proliferation, whereas the PI3K/AKT inhibitor LY294002 primarily inhibited endothelial cell migration; both inhibitors together blocked endothelial cell formation. Taken together, these results supported the use of the TiO_2 nanostructure surface to effectively modulate macrophage polarization and produce a beneficial immune microenvironment for endothelialization. Additional studies are needed to verify the results of this work in vivo.

Conclusion

Our results demonstrated that TiO_2 nanotubes regulated macrophage polarization. Macrophages on the TiO_2 nanotube surface tended toward M2 polarization, particularly for the TNT60 group, with lower production of pro-inflammatory cytokines and higher expression levels of VEGF. In addition, M2 macrophages on the TiO_2 nanotube surface facilitated endothelialization of HUVECs via the ERK1/2 and PI3K/AKT pathways. Therefore, we consider TiO_2 nanotubes a promising candidate for heart valve implants to achieve favorable, rapid endothelialization induced by activated macrophages.

Acknowledgment

This work was funded by the National High-tech Research and Development Program (863 Program) of China (grant no 2014AA020539), the National Natural Science Foundation of China (grant nos 81770388, 81860079, and 81660070), the Outstanding Young Talent Program of Jiangxi Province (grant no 20162BCB23059), the Natural Science Foundation of Jiangxi Province (grant nos 20151BAB205007, 20161BBI90015, and 20171ACB21061), and the Research Project of Jiangxi Provincial Department of Education (grant no 150274).

Author contributions

Wei-Chang Xu and Xiao Dong carried out the experiments. Chao Lu and Jue-Sheng Yang prepared the manuscript. Jian-Liang Zhou and Ji-Chun Liu designed the experiments. Jian-Jun Xu, Yan-Hua Tang, and Ying-Ping Yi analyzed the experimental results. Yi Gong and Wei Yang revised the manuscript. All authors reviewed the manuscript. All authors contributed to data analysis, drafting or revising the article, gave final approval of the version to be published, and agree to be accountable for all aspects of the work.

Disclosure

The authors report no conflicts of interest in this work.

References

1. Joint Task Force on the Management of Valvular Heart Disease of the European Society of Cardiology (ESC), European Association for Cardio-Thoracic Surgery (EACTS); Vahanian A, et al. Guidelines on the management of valvular heart disease (version 2012). *Eur Heart J*. 2012;33(19):2451–2496.
2. de Mel A, Jell G, Stevens MM, Seifalian AM. Biofunctionalization of biomaterials for accelerated in situ endothelialization: a review. *Biomacromolecules*. 2008;9(11):2969–2979.
3. Li G, Yang P, Qin W, Maitz MF, Zhou S, Huang N. The effect of coimmobilizing heparin and fibronectin on titanium on hemocompatibility and endothelialization. *Biomaterials*. 2011;32(21):4691–4703.
4. Rossetti FF, Bally M, Michel R, Textor M, Reviakine I. Interactions between titanium dioxide and phosphatidyl serine-containing liposomes: formation and patterning of supported phospholipid bilayers on the surface of a medically relevant material. *Langmuir*. 2005;21(14):6443–6450.
5. Kulkarni M, Mazare A, Gongadze E, et al. Titanium nanostructures for biomedical applications. *Nanotechnology*. 2015;26(6):062002.
6. Hu Y, Cai K, Luo Z, et al. TiO2 nanotubes as drug nanoreservoirs for the regulation of mobility and differentiation of mesenchymal stem cells. *Acta Biomater*. 2012;8(1):439–448.
7. Neacsu P, Mazare A, Schmuki P, Cimpean A. Attenuation of the macrophage inflammatory activity by TiO_2 nanotubes via inhibition of MAPK and NF-κB pathways. *Int J Nanomedicine*. 2015;10:6455–6467.
8. Fan X, Fan J, Hu X, et al. Preparation and characterization of Ag deposited and Fe doped TiO2 nanotube arrays for photocatalytic hydrogen production by water splitting. *Ceram Int*. 2014;40(10):15907–15917.
9. Prakasam HE, Shankar K, Paulose M, Varghese OK, Grimes CA. A new benchmark for TiO_2 nanotube array growth by anodization. *J Phys Chem C*. 2007;111(20):7235–7241.
10. Beltrán-Partida E, Valdéz-Salas B, Moreno-Ulloa A, et al. Improved in vitro angiogenic behavior on anodized titanium dioxide nanotubes. *J Nanobiotechnology*. 2017;15(1):10.
11. Tan AW, Liau LL, Chua KH, Ahmad R, Akbar SA, Pingguan-Murphy B. Enhanced in vitro angiogenic behaviour of human umbilical vein endothelial cells on thermally oxidized TiO_2 nanofibrous surfaces. *Sci Rep*. 2016;6(1):21828.
12. Wu Q, Li J, Zhang W, et al. Antibacterial property, angiogenic and osteogenic activity of Cu-incorporated TiO_2 coating. *J Mater Chem B*. 2014;2(39):6738–6748.
13. Zhong S, Luo R, Wang X, et al. Effects of polydopamine functionalized titanium dioxide nanotubes on endothelial cell and smooth muscle cell. *Colloid Surface B*. 2014;116:553–560.
14. Thrivikraman G, Madras G, Basu B. In vitro/in vivo assessment and mechanisms of toxicity of bioceramic materials and its wear particulates. *RSC Advances*. 2014;4(25):12763–12781.
15. Asri RIM, Harun WSW, Samykano M, et al. Corrosion and surface modification on biocompatible metals: a review. *Mater Sci Eng C Mater Biol Appl*. 2017;77:1261–1274.
16. Wilson CJ, Clegg RE, Leavesley DI, Pearcy MJ. Mediation of biomaterial-cell interactions by adsorbed proteins: a review. *Tissue Eng*. 2005;11(1–2):1–18.
17. Li J, Chen J, Kirsner R. Pathophysiology of acute wound healing. *Clin Dermatol*. 2007;25(1):9–18.
18. Eming SA, Hammerschmidt M, Krieg T, Roers A. Interrelation of immunity and tissue repair or regeneration. *Semin Cell Dev Biol*. 2009;20(5):517–527.
19. Martinez FO, Sica A, Mantovani A, Locati M. Macrophage activation and polarization. *Front Biosci*. 2008;13(13):453–461.
20. Tarique AA, Logan J, Thomas E, Holt PG, Sly PD, Fantino E. Phenotypic, functional, and plasticity features of classical and alternatively activated human macrophages. *Am J Respir Cell Mol Biol*. 2015;53(5):676–688.
21. Jung SH, Hwang JH, Kim SE, Kim YK, Park HC, Lee HT. Human galectin-9 on the porcine cells affects the cytotoxic activity of M1-differentiated THP-1 cells through inducing a shift in M2-differentiated THP-1 cells. *Xenotransplantation*. 2017;24(4):e12305.
22. Kang H, Zhang J, Wang B, et al. Puerarin inhibits M2 polarization and metastasis of tumor-associated macrophages from NSCLC xenograft model via inactivating MEK/ERK 1/2 pathway. *Int J Oncol*. 2017;50(2):545–554.
23. Wu WK, Llewellyn OP, Bates DO, Nicholson LB, Dick AD. IL-10 regulation of macrophage VEGF production is dependent on macrophage polarisation and hypoxia. *Immunobiology*. 2010;215(9–10):796–803.
24. Zarif JC, Yang W, Hernandez JR, Zhang H, Pienta KJ. The identification of macrophage-enriched glycoproteins using glycoproteomics. *Mol Cell Proteomics*. 2017;16(6):1029–1037.
25. Galas RJ, Liu JC. Surface density of vascular endothelial growth factor modulates endothelial proliferation and differentiation. *J Cell Biochem*. 2014;115(1):111–120.
26. Park H, Kim H-G, Choi W-Y. Characterizations of highly ordered TiO_2 nanotube arrays obtained by anodic oxidation. *Transactions on Electrical and Electronic Materials*. 2010;11(3):112–115.
27. Yeh HI, Lu SK, Tian TY, Hong RC, Lee WH, Tsai CH. Comparison of endothelial cells grown on different stent materials. *J Biomed Mater Res A*. 2006;76(4):835–841.
28. Fukushima K, Miyamoto S, Tsukimori K, et al. Tumor necrosis factor and vascular endothelial growth factor induce endothelial integrin repertories, regulating endovascular differentiation and apoptosis in a human extravillous trophoblast cell line. *Biol Reprod*. 2005;73(1):172–179.
29. Hallab NJ, Jacobs JJ. Chemokines associated with pathologic responses to orthopedic implant debris. *Front Endocrinol*. 2017;8(2):10.
30. Balani K, Verma V, Agarwal A, Narayan R, editors. *Biosurfaces: A Materials Science and Engineering Perspective*. Hoboken, NJ: John Wiley & Sons Inc.; 2015.
31. Brown BN, Ratner BD, Goodman SB, Amar S, Badylak SF. Macrophage polarization: an opportunity for improved outcomes in biomaterials and regenerative medicine. *Biomaterials*. 2012;33(15):3792–3802.
32. Anderson JM, Rodriguez A, Chang DT. Foreign body reaction to biomaterials. *Semin Immunol*. 2008;20(2):86–100.
33. Trindade R, Albrektsson T, Tengvall P, Wennerberg A. Foreign body reaction to biomaterials: on mechanisms for buildup and breakdown of osseointegration. *Clin Implant Dent Relat Res*. 2016;18(1):192–203.
34. Miron RJ, Bosshardt DD. OsteoMacs: Key players around bone biomaterials. *Biomaterials*. 2016;82:1–19.
35. Trindade R, Albrektsson T, Galli S, Prgomet Z, Tengvall P, Wennerberg A. Osseointegration and foreign body reaction: Titanium implants activate the immune system and suppress bone resorption during the first 4 weeks after implantation. *Clin Implant Dent Relat Res*. 2018;20(1):82–91.
36. Hotchkiss KM, Clark NM, Olivares-Navarrete R. Macrophage response to hydrophilic biomaterials regulates MSC recruitment and T-helper cell populations. *Biomaterials*. 2018;182:202–215.
37. Meng S, Liu Z, Shen L, et al. The effect of a layer-by-layer chitosan-heparin coating on the endothelialization and coagulation properties of a coronary stent system. *Biomaterials*. 2009;30(12):2276–2283.
38. Riehle C, Abel ED. MicroRNAs for restenosis and thrombosis after vascular injury. *CircRes*. 2016;118(7):1151–1169.
39. Lin Q, Ding X, Qiu F, Song X, Fu G, Ji J. In situ endothelialization of intravascular stents coated with an anti-CD34 antibody functionalized heparin-collagen multilayer. *Biomaterials*. 2010;31(14):4017–4025.
40. McWhorter FY, Wang T, Nguyen P, Chung T, Liu WF. Modulation of macrophage phenotype by cell shape. *Proc Natl Acad Sci U S A*. 2013;110(43):17253–17258.
41. Pan H, Xie Y, Zhang Z, et al. Immunomodulation effect of a hierarchical macropore/nanosurface on osteogenesis and angiogenesis. *Biomed Mater*. 2017;12(4):045006.
42. Lee CH, Kim YJ, Jang JH, Park JW. Modulating macrophage polarization with divalent cations in nanostructured titanium implant surfaces. *Nanotechnology*. 2016;27(8):085101.
43. Quan H, Kim Y, Park HC, Yang HC. Effects of phosphatidylserine-containing supported lipid bilayers on the polarization of macrophages. *J Biomed Mater Res A*. 2018;106(10):2625–2633.
44. Ma QL, Zhao LZ, Liu RR, et al. Improved implant osseointegration of a nanostructured titanium surface via mediation of macrophage polarization. *Biomaterials*. 2014;35(37):9853–9867.

45. Utomo L, Bastiaansen-Jenniskens YM, Verhaar JA, van Osch GJ. Cartilage degeneration is exacerbated by pro-inflammatory (M1) macrophages but not inhibited by anti-inflammatory (M2) macrophages in vitro. *Osteoarthritis Cartilage*. 2016;24:S34–S35.
46. Loiarro M, Sette C, Gallo G, et al. Peptide-mediated interference of TIR domain dimerization in MyD88 inhibits interleukin-1-dependent activation of NF-κB. *J Biol Chem*. 2005;280(16):15809–15814.
47. Tossetta G, Paolinelli F, Avellini C, et al. IL-1β and TGF-β weaken the placental barrier through destruction of tight junctions: an in vivo and in vitro study. *Placenta*. 2014;35(7):509–516.
48. Amir Levy Y, Ciaraldi TP, Mudaliar SR, Phillips SA, Henry RR. Excessive secretion of IL-8 by skeletal muscle in type 2 diabetes impairs tube growth: potential role of PI3K and the Tie2 receptor. *Am J Physiol Endocrinol Metab*. 2015;309(1):E22–E34.
49. Wang J, Qian S, Liu X, et al. M_2 macrophages contribute to osteogenesis and angiogenesis on nanotubular TiO_2 surfaces. *J Mater Chem B*. 2017;5(18):3364–3376.
50. Ameredes BT, Zamora R, Gibson KF, et al. Increased nitric oxide production by airway cells of sensitized and challenged IL-10 knockout mice. *J Leukoc Biol*. 2001;70(5):730–736.
51. Wang J, Meng F, Song W, et al. Nanostructured titanium regulates osseointegration via influencing macrophage polarization in the osteogenic environment. *Int J Nanomedicine*. 2018;13:4029–4043.
52. Park J-W, Han S-H, Hanawa T. Effects of surface nanotopography and calcium chemistry of titanium bone implants on early blood platelet and macrophage cell function. *Biomed Res Int*. 2018;2018:1–10.
53. Lü WL, Wang N, Gao P, Li CY, Zhao HS, Zhang ZT. Effects of anodic titanium dioxide nanotubes of different diameters on macrophage secretion and expression of cytokines and chemokines. *Cell Prolif*. 2015;48(1):95–104.
54. Yao S, Feng X, Li W, Wang L-N, Wang X. Regulation of RAW 264.7 macrophages behavior on anodic TiO2 nanotubular arrays. *Front Mater Sci*. 2017;11(4):318–327.
55. Rajyalakshmi A, Ercan B, Balasubramanian K, Webster TJ. Reduced adhesion of macrophages on anodized titanium with select nanotube surface features. *Int J Nanomedicine*. 2011;6:1765–1771.
56. Hotchkiss KM, Reddy GB, Hyzy SL, Schwartz Z, Boyan BD, Olivares-Navarrete R. Titanium surface characteristics, including topography and wettability, alter macrophage activation. *Acta Biomater*. 2016;31:425–434.
57. Lisong YIN, Yongping C, Tan M, Ting LI, Hailu FAN. Effection of CH_3COOH treatment on hydrophilicity TiO_2 thin film on glass. *World Sci-Tech R and D*. 2007;29(3):6–9.
58. Anitha VC, Lee JH, Lee J, Banerjee AN, Joo SW, Min BK. Biofilm formation on a TiO_2 nanotube with controlled pore diameter and surface wettability. *Nanotechnology*. 2015;26(6):065102.
59. Cipriano AF, Miller C, Liu H. Anodic growth and biomedical applications of TiO_2 nanotubes. *J Biomed Nanotechnol*. 2014;10(10):2977–3003.
60. Tiller JC, Bonner G, Pan LC, Klibanov AM. Improving biomaterial properties of collagen films by chemical modification. *Biotechnol Bioeng*. 2001;73(3):246–252.
61. Rebl H, Finke B, Ihrke R. Positively charged material surfaces generated by plasma polymerized allylamine enhance vinculin mobility in vital human osteoblastss. *Adv Eng Mater*. 2010;12(8):B356–B364.
62. Wang FQ, Chen G, Zhu JY, et al. M2-polarised macrophages in infantile haemangiomas: correlation with promoted angiogenesis. *J Clin Pathol*. 2013;66(12):1058–1064.
63. Liu YC, Hsiao YY, Ku KL, Liao HF, Chao WC. *Mahonia oiwakensis* extract and its bioactive compounds exert anti-inflammatory activities and VEGF production through M2-macrophagic polarization and STAT6 activation. *J Med Food*. 2018;21(7):654–664.
64. Sevostyanova VV, Antonova LV, Velikanova EA, et al. Endothelialization of polycaprolactone vascular graft under the action of locally applied vascular endothelial growth factor. *Bull Exp Biol Med*. 2018;165(2):264–268.
65. Jin J, Yuan F, Shen MQ, Feng YF, He QL. Vascular endothelial growth factor regulates primate choroid-retinal endothelial cell proliferation and tube formation through PI3K/Akt and MEK/ERK dependent signaling. *Mol Cell Biochem*. 2013;381(1–2):267–272.
66. Li W, Man XY, Li CM, et al. VEGF induces proliferation of human hair follicle dermal papilla cells through VEGFR-2-mediated activation of ERK. *Exp Cell Res*. 2012;318(14):1633–1640.
67. Beierle EA, Nagaram A, Dai W, Iyengar M, Chen MK. VEGF-mediated survivin expression in neuroblastoma cells. *J Surg Res*. 2005;127(1):21–28.